Collective behavior in groups of self-propelled particles with active and passive sensing inspired by animal echolocation

Masoud Jahromi Shirazi and Nicole Abaid

Phys. Rev. E **98**, 042404 — Published 8 October 2018

DOI: 10.1103/PhysRevE.98.042404

Collective behavior in groups of self-propelled particles with active and passive sensing inspired by animal echolocation

Masoud Jahromi Shirazi[1] and Nicole Abaid[1,*]

[1] *Engineering Mechanics Program, Virginia Tech, Blacksburg, VA, 24061 USA*

(Dated: September 19, 2018)

Collective behavior is observed in many physical and biological systems and has been studied through agent-based models, including the Vicsek model which enforces aligned motion among agents. The behaviors produced by these models are highly dependent on the type of sensing individuals use. In nature, bats successfully use a complex form of sensing, namely, active echolocation in a relatively narrow beam and passive eavesdropping on their conspecifics' sound over a wider volume. Inspired by this system, we investigate whether augmenting an active sensing mechanism with passive sensing can improve the collective behavior of the group. A three-dimensional Vicsek-type model is presented to study the effects of combining active and passive sensing on collective behavior of a group of particles in the presence of noise. Phase transition is observed in both the presence and absence of passive sensing, yet the range of parameters for which ordered and disordered group states exist dramatically changes when passive sensing is implemented. Notably, we find numerous cases of the model for which the implementation of passive sensing increases the robustness of the collective behavior to noise.

PACS numbers: 05.65.+b, 87.18.Tt, 64.60.De

I. INTRODUCTION

When a group of individuals interacts among themselves using simple rules, they can exhibit complex behavior as a whole. This phenomenon is referred to as *collective behavior* and has manifested in many physical systems such as vibrating rods [1], nematic liquid crystal [2], and active colloids [3]. It is also observed in living systems such as fish schools [4], bird flocks [5], primates [6], insects [7], cells [8], amoeba [9], bacterial colonies [10], and human crowds [11]. Depending on the rules of motion and interaction between individuals, the group can show different patterns of ordered behavior such as aligned movement or milling.

Modeling collective behavior is a problem that has been approached by researchers from different communities. The agent-based model provided by Vicsek [12], which is commonly referred as the Vicsek model, is one of the most well-studied due to its ability to capture complex group behaviors with a simple update rule. In this model, each agent or particle is moving with constant speed in a two-dimensional square with periodic boundary conditions and, at each time step, the particles take the average direction of their neighboring particles, subjected to noise. The polarization, which is the averaged linear momentum of the group, is considered as an order parameter for aligned movement. As the intensity of the noise increases to some critical value, the order parameter drops dramatically which shows a *phase transition* in the group. A three-dimensional version of the Vicsek model has been more recently published in [13]. The paper published by Chaté et al. expands the Vicsek model by adding polarity to particles and their interaction, as well as including the effect of an ambient fluid and cohesion between nearby particles in both two and three dimensions [14]. Besides the Vicsek model which is based on sensing neighbors' direction of motion, we note that collective behavior may be seen in models that use alternative sensing strategies, see for example the position-based model in [15]. A thorough review of collective motion, its manifestation in different research areas, and different suggested models can be found in [16].

The behavior of particles in the Vicsek model is highly dependent on their ability to sense their environment. Inspired by sensory limitations in biological and robotic systems, recent models have sought to explore the role of a so-called *sensing angle*. This angle defines the portion of the circular/spherical neighborhood around an agent that it can perceive, and thus the information it can use for the alignment protocol. In addition to the phase transition that can be found by changing noise on alignment, the relationship between sensing angle and polarization is still an active area of research. Nguyen et al. demonstrate a phase transition with changing sensing angle in the two-dimensional Vicsek model [17], with the critical noise value defined where polarization variance is maximized over different sensing angles. They report that the critical noise increases with increasing sensing angle. Also, they show by simulation that the critical noise converges to some value as the number of agents increases and this value is negligible for angles less than $\frac{\pi}{2}$. Therefore, no phase transition with respect to noise happens for the case with sensing angle is less than $\frac{\pi}{2}$. Durve and Sayeed use the same model to study polarization as sensing angle is varied [18]. The authors find that the phase transition is of the first order when sensing angle is varied, while it is of the second order when the radius of the circular neighborhood around the particle is varied. In

* nabaid@vt.edu

[19], the two-dimensional deterministic Vicsek-like model with angle restriction is considered and an optimal angle is found which leads to the fastest alignment of particles. The three-dimensional version of this problem is also considered in [20], however the final results are hard to interpret since the equations may be written in two rather than three dimensions. Decoupling the directions of sensing and motion may also lead to significant decreases in the time to align, as is shown in [21].

Vicsek-like agent-based models are often used to capture collective behavior in animal groups and their engineered analogs, robotic swarms. To interact with and gather information from the environment, individuals rely on sensing mechanisms. These mechanisms can use different signals such as light [5], sound [22], chemicals [23], and electrical charge [24]. Sensors can be categorized in two different groups, *active sensors* and *passive sensors*. Active sensors use energy to create a signal and gather information about the environment from its reflection. Radar, sonar, and lidar are examples of active sensors. In contrast, passive sensors analyze signals already present in the environment [25]. Cameras, microphones, and thermometers are examples of passive sensors. Since many animal groups rely on passive sensing, such as vision, most models for biological systems are designed with only passive sensing. In contrast, groups that use active sensing may have different communication modalities since their sensing signals are broadcast and thus interceptable by design.

Bat swarms are an example of highly successful animal groups that use active sensing, that is, echolocation for navigation [22]. Collective behavior using active sensing comes with unique features, as are reported in bats. As an example, it is known that bats use different calls with different beam patterns to get a balance between range, breadth, and resolution of sensing [26]. Therefore they have the ability to control their sensing range and sensing angle. Another example of a feature unique to active sensing is the interference of the reflected signals made by different bats in the group, sometimes referred to as *jamming*. Bats use different strategies such changing sound frequency [27], temporal characteristics of the sound [28], direction of the sound [29] or even flying without echolocating [30]. A summary of the research done on bats and whale echolocation can be found in [26].

The silent flight of bats observed in [30], which the authors suggest may prevent jamming, raises the question of how bats can maneuver and avoid obstacles during their silent flight. One possible answer to this question is that they interact with the environment through eavesdropping on the sound made by other bats. In other words, bats are able to combine passive listening, i.e. sound source localization, with active echolocation. Given the fact that bats can also change the sensing angle of their active sensing, we may ask how can changing the sensing angle and using passive sensing impact the collective behavior of the group.

Inspired by bats' sensing, this study seeks to investigate whether augmenting an active sensing mechanism with passive sensing can improve the collective behavior of the group. We study the collective behavior of a group of particles using both active and passive sensing in the presence of noise through a three-dimensional agent-based model in the spirit of Vicsek. Using polarization as an order parameter, we study phase transitions evidencing collective behavior as noise magnitude and sensing angle change.

II. SELF-PROPELLED PARTICLE MODEL

The self-propelled particle model consists of N particles moving in a three-dimensional cubic domain of length L with constant speed v_0. The boundary condition of the cube is assumed to be periodic. Each particle has a spherical sensing space with radius R. This sensing space is split up into an active sensing region, i.e. points inside a cone with opening angle 2θ, and a passive sensing region which covers all the points outside the active sensing cone. All the particles within distance R of a specific particle, including the particle itself, are called its *neighbors*. Whether a neighbor is located inside the cone of active sensing or outside of it can be used to divide the neighbors into two disjoint sets which we call *active neighbors* and *passive neighbors*, respectively. The particle itself is considered to be an active neighbor. This geometric partitioning of neighbors is inspired by the angular limitation of active sonar, which occurs in a fairly narrow beam, while passive sonar can be performed omnidirectionally.

Particle i at time step k has position vector $\mathbf{x}_i\,(k)$ and heading vector $\mathbf{v}_i\,(k)$, which is a unit vector defining the direction of motion of the particle. At time step $k+1$, this particle assumes the following heading vector:

$$\mathbf{v}_i(k+1) = \mathbf{N}\left(\frac{n_{\mathrm{a}}\mathbf{v}_i^{\mathrm{a}}(k+1) + n_{\mathrm{p}}\mathbf{v}_i^{\mathrm{p}}(k+1)}{n_{\mathrm{a}}+n_{\mathrm{p}}}\right), \quad (1)$$

where n_{a} and n_{p} are the number of active and passive neighbors, respectively, and $\mathbf{N}\,(\mathbf{u}) = \mathbf{u}/\|\mathbf{u}\|$ returns a unit vector in the direction of vector $\mathbf{u}$. Finally, $\mathbf{v}_i^{\mathrm{a}}(k+1)$ and $\mathbf{v}_i^{\mathrm{p}}(k+1)$ model the contribution of the active and passive neighbors' headings in the particle's heading direction, which are calculated as follows:

$$\mathbf{v}_i^{\mathrm{a}}(k+1) = \mathbf{N}\left(\mathbf{N}\left(\sum_{j\in\Lambda_i^{\mathrm{a}}(k)}\mathbf{v}_j(k)\right) + \xi_{\mathrm{a}}(k)\right), \quad (2)$$

$$\mathbf{v}_i^{\mathrm{p}}(k+1) = \mathbf{N}\left(\mathbf{N}\left(\sum_{j\in\Lambda_i^{\mathrm{p}}(k)}\mathbf{v}_j(k)\right) + \xi_{\mathrm{p}}(k)\right), \quad (3)$$

where $\Lambda_i^{\mathrm{a}}(k)$ and $\Lambda_i^{\mathrm{p}}(k)$ are index sets of active and passive neighbors, respectively. The noise vectors $\xi_{\mathrm{a}}(k)$

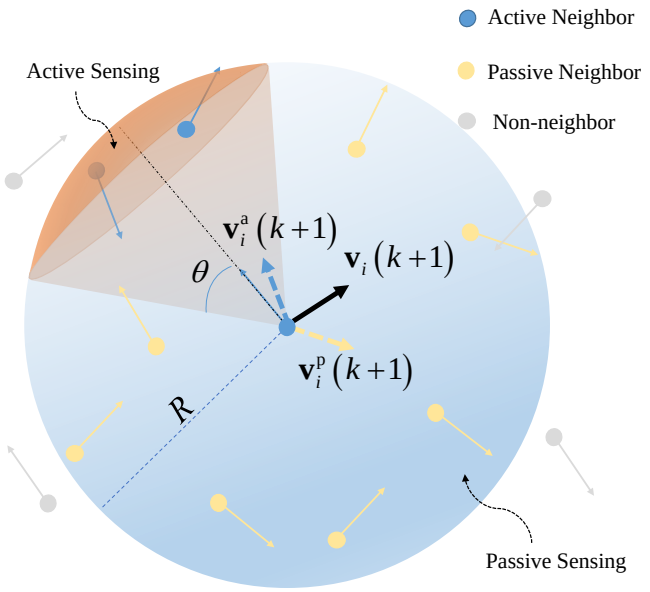

FIG. 1: A schematic of a particle and its active and passive neighbors. Blue and yellow dashed vectors show the average heading of active and passive neighbors, respectively, and the calculated heading of the particle at next time step is shown as a black vector.

and $\xi_{\mathrm{p}}(k)$ are random vectors uniformly distributed over spheres with radii η_{a} and η_{p}, respectively.

According to equation (1), each particle assumes a weighted average of the heading of its neighboring particles as its new heading direction. In other words, each particle calculates the heading of its neighbors using active and passive sensing separately, disturbed by a noise. The particle then computes the heading direction for the next time step by assigning a weight to each direction based on the number of active and passive neighbors. A schematic of the heading direction update is depicted in figure 1.

The average heading vectors of active and passive neighbors are disturbed by noises $\xi_{\mathrm{a}}(k)$ and $\xi_{\mathrm{p}}(k)$, respectively. These noise vectors, that we call *active noise* and *passive noise*, are assumed to be uniformly distributed over spheres of radii η_{a} and η_{p}, respectively. The two noises are used to model incapability of the particle to head exactly toward the average heading vector of the active or passive neighbors due to muscle or actuation resolution. This randomness can also be seen as the particle's *free will* to deviate from the average heading of the neighbors based on the particle's *trust* in its neighbors or in the accuracy of its sensing. Since the particle interacts with active and passive neighbors via different sensing approaches, it is rational to consider different values for active noise and passive noise to model different levels of trust in these approaches.

The modeling selection of differentiating between active and passive sensing through the separate, randomly perturbed updates in equations (2) and (3) seeks to capture behavioral responses inspired by bats' use of echolocation and eavesdropping. These two types of sensing result in information which is known to be more or less accurate by design. The physics of active and passive sensing is incorporated into the choice of geometry for the sensing regions. The relative trust in the accuracy of information from active and passive sensing is incorporated into the noises ξ_{a} and ξ_{p}. However, the model is not intended to capture the physics and biology governing active or passive sensing, instead focusing on the relationship between individual and collective behavior in groups of particles.

Once the heading vector of particle i in the next time step is calculated, the updated position of this particle can be found as

$$\mathbf{x}_i(k+1) = \mathbf{x}_i(k) + v_0 \mathbf{v}_i(k+1). \tag{4}$$

It should be noted here that since each particle is assumed to be its own active neighbor, n_{a} is at least one and therefore, equation (1) is well defined. Also, in the special case when $\theta = \pi$, all the neighbors are active and the model is reduced to the three-dimensional version of the Vicsek model with noise strength η_{a}. When $\theta = 0$, however, this model will not recover the Vicsek model since the particle itself is an active neighbor and the noise term in equation (2) will be added to that in equation (3), and the resulting noise will not be uniformly distributed over a sphere.

To study the collective behavior of the group, we consider the order parameter of *polarization*, which is the magnitude of the averaged group linear momentum. Polarization of a group of particles can be defined as

$$P(k) = \frac{1}{N} \left\| \sum_{i=1}^{N} \mathbf{v}_i(k) \right\|. \tag{5}$$

Polarization is a real number between zero and one, where larger values indicate higher alignment in the group. When the value of polarization is equal to one, it is associated with a perfectly aligned group, while polarization close to zero shows that the particles are performing random walks.

III. SIMULATIONS

After defining the model, numerical simulation is used to investigate the effect of active sensing noise amplitude η_{a}, sensing angle θ, and passive sensing noise amplitude η_{p} on the polarization. The model considers particles moving in three dimensions inside a cube with length $L = 15$. All particles have a sensing range of $R = 1$ and are moving with constant speed $v_0 = 0.03$. The average density, which is equal to the number of particles per unit volume, is set to be equal to one. We vary two control parameters, η_{a} and θ, for different values of η_{p}. Simulations

are done for 5 different cases: $\eta_{\rm p} = \{0, 0.6, 1.2, 1.8\}$ and no passive sensing, which refers to the case when particles use only active sensing, i.e. $v_i(k+1) = v_i^{\rm a}(k+1)$. The sensing angle θ changes from zero to π, with increment of $\pi/36$, and $\eta_{\rm a}$ takes values between 0 and 1.8, with increment of 0.2. For each simulation, the model is iterated in time until it reaches to a stationary condition. Rigorously, we consider the polarization to be stationary if it satisfies the first-order weak stationarity condition, in which the first moment of polarization remains constant [31]. After omitting 30,000 time steps to capture the transient, the polarization is averaged over moving windows of length 30,000 time steps which proceed with an increment of 100 time steps. To test whether the average polarization over the moving windows is constant, we compute the coefficient of variation of these values. This quantity does not exceed 7% for all considered simulation parameters, which we take to satisfy the qualitative definition of stationarity above. Simulation parameters are condensed in table I. For the analysis below, we report the mean polarization averaged over all time steps after the omitted transient for each set of simulation parameters.

Variable	**Symbol**	**Value**
Cubic domain side length	L	15
Density of particles	ρ	1
Number of particles	N	3375
Particle speed	v_0	0.03
Sensing range (linear)	R	1
Sensing angle	θ	$[0, \pi]$
Passive sensing noise amplitude	$\eta_{\rm p}$	$\{0, 0.6, 1.2, 1.8\}$ and None
Active sensing noise amplitude	$\eta_{\rm a}$	$\{0, 0.2, \ldots, 1.8\}$
Total simulation time steps	K	300,000
Time steps omitted as transient	-	30,000

TABLE I: Simulation parameters

IV. RESULTS AND DISCUSSION

The averaged polarization of the group is shown in figure 2 as a function of sensing angle and active noise magnitude for different conditions of passive sensing. In all considered cases of passive sensing, when the sensing angle is π, the trend of the model is consistent with the three-dimensional Vicsek model. Namely, the polarization is high for small values of $\eta_{\rm a}$, and decreases to zero with increasing noise. Also, at any fixed sensing angle and passive sensing condition, the polarization decreases monotonically as $\eta_{\rm a}$ increases. Moreover, when the sensing angle is fixed, at any active noise magnitude, the polarization decreases as the magnitude of passive noise increases. As either noise is increased beyond a critical value, the polarization appears to approach a limit.

The four plots in figure 2 show the effects of adding passive sensing with different $\eta_{\rm p}$ to the active sensing with restricted angle. In contrast to the effect of passive noise, there are some values of $\eta_{\rm a}$ for which polarization shows a maximum with increasing θ. This occurs when the active noise does not dominate passive noise, that is, when $\eta_{\rm a}$ is either less than or approximately equal to $\eta_{\rm p}$. The white circles show the locations of maxima in polarization for fixed values of $\eta_{\rm a}$ as θ is varied. For sets of simulations with fixed $\eta_{\rm a}$ where no averaged polarization was above one standard deviation of all other simulations in the set, we did not report the maximum. These cases generally referred to averaged polarizations that were constant or changed monotonically as theta increased.

Figure 3 shows the case with no passive sensing. When the sensing angle is less than a threshold, approximately equal to $\pi/2$, the ordered phase exists only at very small values of $\eta_{\rm a}$. This is similar to results reported by [17] in which they show that in the two-dimensional Vicsek model with variable sensing angle, for angles smaller than $\pi/2$, the critical noise is very small and the ordered phase does not practically exist. As the sensing angle increases above this threshold, the range of active noise magnitude where the ordered phase exists ($P \backsimeq 1$) dramatically increases. In other words, if the magnitude of noise is not too large, there is a sharp phase transition as the sensing angle increases. This sharp phase transition is also reported for two-dimensional model in [18]. Moreover, the phase transition as the sensing angle increases in the presence of passive sensing (figure 2) appears more gradual in comparison to the phase transition when particles only use active sensing in figure 3. Moreover, the range of active noise in which the ordered phase exists is not monotonically increasing with θ and shows some optimal sensing angle. In other words, the optimal sensing angle is associated with a system whose order is more robust to the introduction of active noise. This is similar to the results reported in [19] for the two-dimensional Vicsek model, except they defined optimality based on how fast polarization reaches to 1 when there is no noise in the model. For small values of active noise magnitude, e.g. $\eta_{\rm a} < 0.6$, phase transition occurs with respect to increasing θ, while for larger values of active noise magnitude, the phase transition is absent since the ordered phase is never reached.

In the presence of passive noise, however, the polarization does not monotonically increase as the sensing angle increases for all value of active noise magnitude. When particles use passive sensing and active sensing together, depending on the relative values of active noise magnitude and passive noise magnitude, the collective behavior can be divided into three different cases: $\eta_{\rm p} >> \eta_{\rm a}$, $\eta_{\rm p} \backsimeq \eta_{\rm a}$, and $\eta_{\rm p} << \eta_{\rm a}$. In the first case, when the sensing angle is large, the behavior of the system is similar to the case with no passive sensing since the number of passive neighbors is negligible comparing to the number of active neighbors. At smaller sensing angles, however, especially when the active noise is not close to zero, exploiting

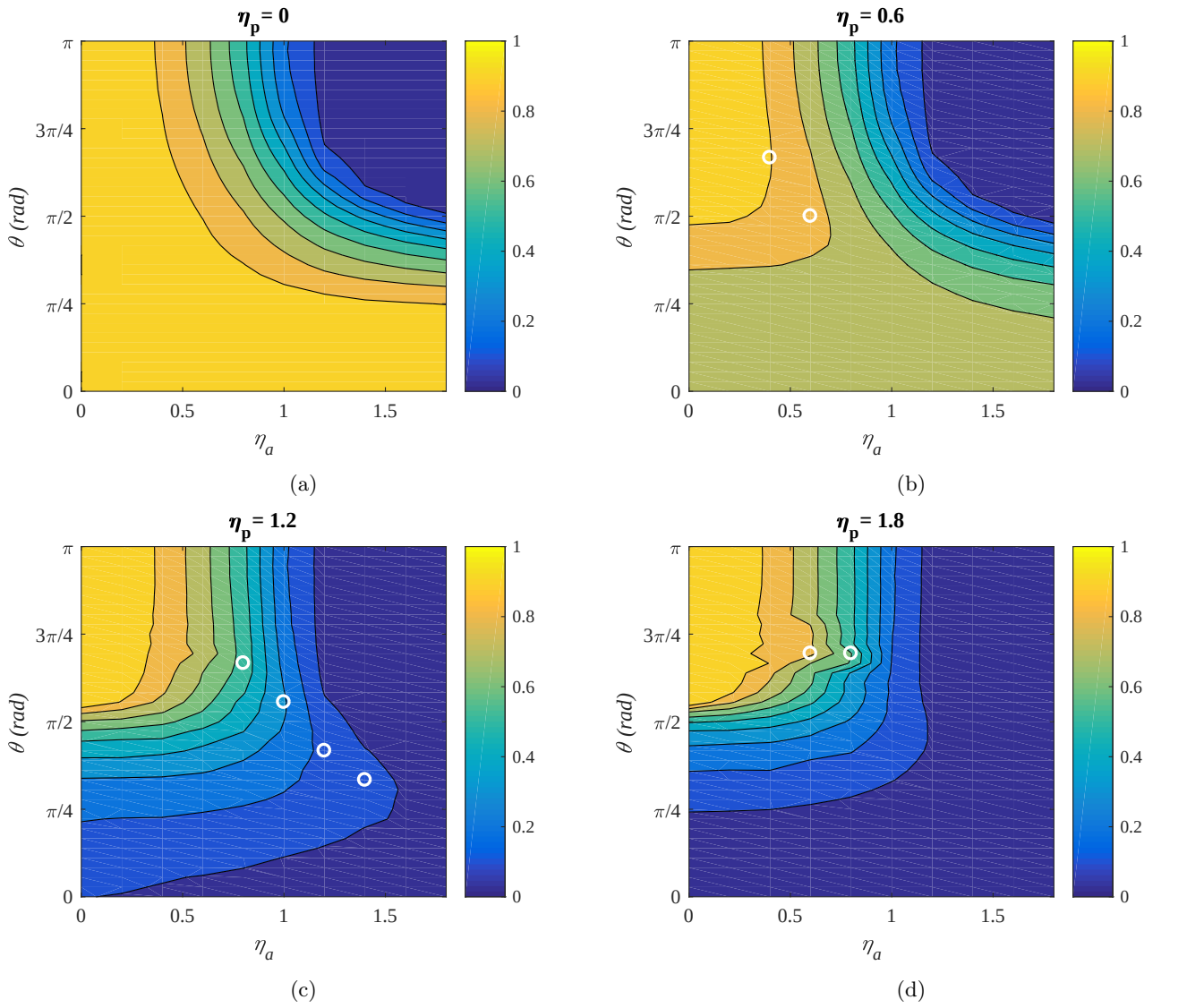

FIG. 2: Averaged polarization as a function of sensing angle and active noise amplitude for different values of passive noise amplitude. The white circles shows the maximum value of polarization for fixed η_a.

passive sensing improves polarization of the group compared to the no-passive-sensing case. For example, the polarization when $\eta_a = 0.4$ and $\theta = \pi/4$ is 0.7776 when $\eta_p = 0.6$ and 0.0748 when no passive sensing is allowed. This order-of-magnitude improvement to system order is due to extra information that is ignored when using only active sensing. It is notable that this boost occurs even though the extra information from passive sensing is noisy compared to its active counterpart.

For the second case When active noise magnitude and passive noise magnitude are close to each other, according to equations (1)-(3), the effective noise acting on the system is the sum of two zero-mean noises which are uniformly distributed over the sphere and therefore, their summed effect has a smaller magnitude compared to those of the original summands. As a result, the maximum polarization occurs at more restricted angles compared to the no passive sensing case. This effect of averaging zero-mean noises can be seen by considering the line plots in figure 4, which uses $\eta_p = 1.2$ and captures vertical slices of figure 2(c) at $\eta_a = 0.8, 1, 1.2$, and 1.4. The maxima of polarization occur at approximately $\theta = 2.182, 1.658, 1.309$ and 1.047 rad respectively. This behavior is expected since, as the particle's trust of its active neighbors decreases, it relies more on passive neighbors to get more information necessary for alignment, which is achieved by reducing the sensing angle.

For the third case when passive noise is much smaller than active noise, the interpretation of the noises as trust of the sensing process means that passive sensing is trusted dominantly over active sensing by the particle. Therefore, the polarization increases as the sensing

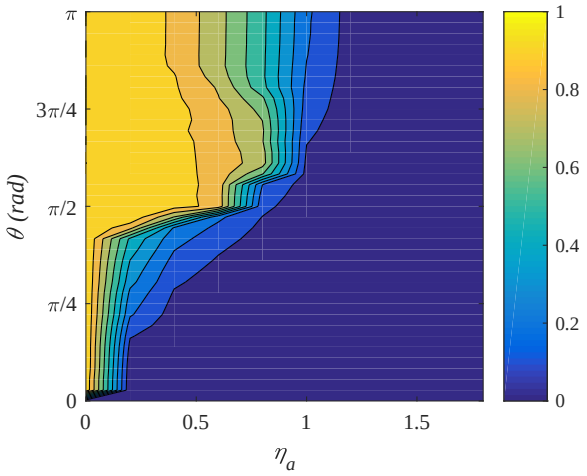

FIG. 3: Averaged polarization as a function of sensing angle and active noise amplitude when only active sensing is implemented.

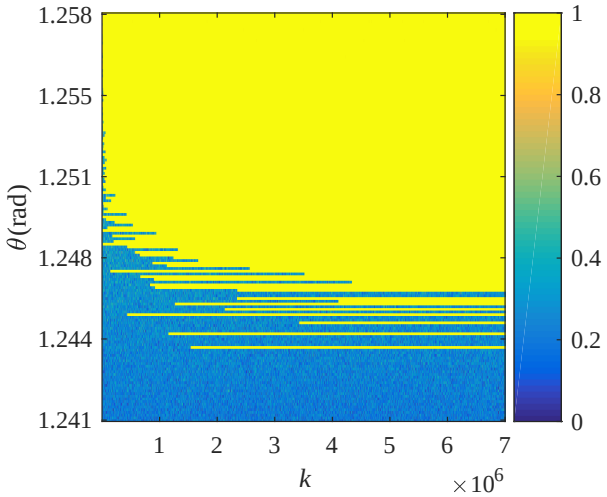

FIG. 5: Time series of the instantaneous polarization near critical sensing angle at $\eta_{\rm a} = 0.4$ for 150 different values of sensing angle with resolution 0.0035 radians.

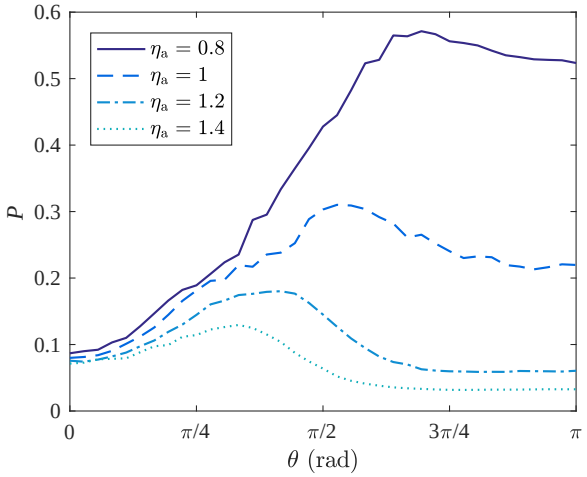

FIG. 4: Averaged polarization at different active noise amplitude as a function of sensing angle when $\eta_{\rm p} = 1.2$

angle decreases, and more neighbors are passive neighbors than active. The level curves of polarization in this case are interesting. As it can be seen in figure 2(a), the larger sensing angle with smaller active noise has the same polarization as smaller sensing angle with larger active noise. It can be interpreted as a trade off between using too many active neighbors with moderate active noise versus a group of less active neighbors with strong noise condition and a group of passive neighbors with small noise. Moreover, it seems that as active noise magnitude increases, the polarization approaches a limit at each sensing angle. This occurs because, when the active noise magnitude is high, the sum of the direction of the active neighbors will be negligible compared to the active noise vector. In other words, the information gathered by active neighbors is so corrupted by noise that it is effectively just random with no useful information.

As an interesting side note, comparison between polarization in the no passive sensing case of figure 3 and all the cases fusing active and passive sensing in figures 2a-2d suggests that, in presence of passive sensing, the phase transition is happening more gradually as the sensing angle changes compared to the no passive sensing case. One explanation for this difference could be that the extra information gathered with the additional use of passive sensing requires particles to perform more averaging, which makes the phase transition from disorder to order emerge more smoothly. However, due to finite size of the domain for the simulated system, determining the location and nature of phase transition is difficult. A common tool to rigorously investigate this matter is finite size scaling analysis [32]. However, its implementation requires a large domain size to be simulated over a long period of time. Since our model is three dimensional, the number of particles is proportional to L^3, which makes employing finite size analysis infeasible due to computational demands. In [18], the nature of the phase transition as the sensing angle changes is detected as first-order in the two-dimensional case, however, for the three-dimensional model, a through investigation similar to the analysis in [14] is required, which is beyond the scope of this work. Being aware of the finite size effects, one can qualitatively describe the phase transition. Figure 5 shows the polarization time series for the case with no passive sensing stacked for 150 different values of sensing angle around the phase transition with resolution of 0.0035 radians, at $\eta_{\rm a} = 0.4$. When the sensing angle is less than critical value, polarization is uniformly low, and as this angle increases above a critical value, polarization is uniformly

high. However, between these two unimodal states, the system sometimes converges to the ordered phase and if it does, the time it takes to reach the ordered phase is significantly longer than the transient as defined by our notion of stationarity. This can be a sign of the coexistence of ordered and disordered states, however, we failed to observe bimodality in contrast to what reported in two-dimensional model in [18]. In summary, whether the phase transition in the three-dimensional Vicsek model with no passive sensing is first-order and whether implementing passive sensing will change the nature of phase transition requires a more thorough investigation which will be explored in future studies of this model.

V. CONCLUSION

Inspired by bats' active sensing and eavesdropping, a three-dimensional Vicsek-type model is introduced to study the effects of using active and passive sensing with restricted sensing angle on collective behavior of a group of individuals in the presence of noise. The range of parameters for which the ordered phase exists changes when passive sensing is introduced to the model. Also, at different values of active and passive noise amplitude, the maximum polarization happens at different sensing angles. Moreover, while the phase transition is sharp when only active sensing is implemented, it is noticeably smoother when passive sensing is added to the model.

VI. ACKNOWLEDGEMENTS

This work was supported by the National Science Foundation under grants CMMI-1751498 and CMMI-1342176.

[1] D. L. Blair, T. Neicu, and A. Kudrolli, Physical Review E **67**, 031303 (2003).
[2] V. Narayan, S. Ramaswamy, and N. Menon, Science **317**, 105 (2007).
[3] I. S. Aranson, Physics-Uspekhi **56**, 79 (2013).
[4] B. L. Partridge, Scientific American **246**, 114 (1982).
[5] I. L. Bajec and F. H. Heppner, Animal Behaviour **78**, 777 (2009).
[6] C. Sueur and O. Petit, International Journal of Primatology **29**, 1085 (2008).
[7] I. D. Couzin and N. R. Franks, Proceedings of the Royal Society of London B: Biological Sciences **270**, 139 (2003).
[8] T. Surrey, F. Nédélec, S. Leibler, and E. Karsenti, Science **292**, 1167 (2001).
[9] D. A. Kessler and H. Levine, Physical Review E **48**, 4801 (1993).
[10] C. Dombrowski, L. Cisneros, S. Chatkaew, R. E. Goldstein, and J. O. Kessler, Physical Review Letters **93**, 098103 (2004).
[11] E. Bonabeau, Proceeding of the National Academy of Sciences of the United States **99**, 72807287 (2002).
[12] T. Vicsek, A. Czirók, E. Ben-Jacob, I. Cohen, and O. Shochet, Physical Review Letters **75**, 1226 (1995).
[13] A. Czirók, M. Vicsek, and T. Vicsek, Physica A: Statistical Mechanics and its Applications **264**, 299 (1999).
[14] H. Chaté, F. Ginelli, G. Grégoire, F. Peruani, and F. Raynaud, The European Physical Journal B **64**, 451 (2008).
[15] L. Barberis and F. Peruani, Physical Review Letters **117**, 248001 (2016).
[16] T. Vicsek and A. Zafeiris, Physics Reports **517**, 71 (2012).
[17] P. T. Nguyen, S.-H. Lee, and V. T. Ngo, Physical Review E **92**, 032716 (2015).
[18] M. Durve and A. Sayeed, Physical Review E **93**, 052115 (2016).
[19] B.-M. Tian, H.-X. Yang, W. Li, W.-X. Wang, B.-H. Wang, and T. Zhou, Physical Review E **79**, 052102 (2009).
[20] Y.-J. Li, S. Wang, Z.-L. Han, B.-M. Tian, Z.-D. Xi, and B.-H. Wang, EPL (Europhysics Letters) **93**, 68003 (2011).
[21] X. Zhang, S. Jia, and X. Li, Nonlinear Dynamics **90**, 43 (2017).
[22] N. I. Hristov, L. C. Allen, and B. A. Chadwell, "New advances in the study of group behavior in bats," in *Bat Evolution, Ecology, and Conservation*, edited by R. A. Adams and S. C. Pedersen (Springer New York, New York, NY, 2013) Chap. 14, pp. 271–291.
[23] J.-L. Deneubourg, S. Aron, S. Goss, and J. M. Pasteels, Journal of Insect Behavior **3**, 159 (1990).
[24] G. W. M. Westby, Science Progress **69**, 291 (1984).
[25] H. I. Christensen and G. D. Hager, "Sensing and estimation," in *Springer Handbook of Robotics*, edited by B. Siciliano and O. Khatib (Springer, New York, NY, 2016) Chap. 5, pp. 91–112.
[26] A. Surlykke, P. E. Nachtigall, R. R. Fay, and A. N. Popper, eds., *Biosonar* (Springer, 2014).
[27] M. E. Bates, S. A. Stamper, and J. A. Simmons, Journal of Experimental Biology **211**, 106 (2008).
[28] M. K. Obrist, Behavioral Ecology and Sociobiology **36**, 207 (1995).
[29] C. Chiu, P. V. Reddy, W. Xian, P. S. Krishnaprasad, and C. F. Moss, Journal of Experimental Biology **213**, 3348 (2010).
[30] C. Chiu, W. Xian, and C. F. Moss, Proceedings of the National Academy of Sciences **105**, 13116 (2008).
[31] W. Yang and I. Zurbenko, Wiley Interdisciplinary Reviews: Computational Statistics **2**, 107 (2010).
[32] V. Privman, *Finite Size Scaling and Numerical Simulation of Statistical Systems* (World Scientific, 1990).